Signal Propagation Modelling for Vehicle-To-Infrastructure Communication Under the Influence of Metal Obstruction

J S C Turner[1,2] , A B Shahriman[1, 3] , A Harun[1, 2*] , M S M Hashim[1, 3] , Z M Razlan[1,3] , D L Ndzi[4] , R C Ismail[2] , S A Z Murad[2] , M N M Isa[2] , S N Mohyar[2] , M F Ramli[2] and M K N Zulkifli[2]

[1]Center of Excellence Automotive & Motorsport, Universiti Malaysia Perlis, Malaysia
[2]Faculty of Electronic Engineering Technology, Universiti Malaysia Perlis, Malaysia
[3]Faculty of Mechanical Engineering Technology, Universiti Malaysia Perlis, Malaysia
[4]University West of Scotland, United Kingdom

ABSTRACT

Connected car has become one of emerging technology in the automotive industries today. This development preludes a rise in vehicular communication studies that primarily targets radio channel modelling on vehicle-to-vehicle (V2V) and vehicle-to-infrastructure (V2I) communication mode. Considering vehicular obstruction, vast channel propagation studies have focused more on V2V mode while others consider the typical urban scenarios consisting of high traffic volumes of moving vehicles. Due to challenging propagation mechanisms and high complexity in such areas, radio propagation models applied in simulators assume an obstacle-free environment rather than considering the least effect imposed by metal obstruction on communication signal. Besides, there are limited studies pertaining to metal obstruction that considers several under-explored environments such as actual parking lots, junctions and other road infrastructure support. As such, this paper demonstrates signal attenuation analysis caused by the presence of metal objects in low density over obstacle-free environment on actual parking lot via V2I mode. Two scenarios such as LOS and NLOS conditions consisting of obstacle-free, cars and buses as static metal objects are evaluated. The aim of this research is to characterize signal strength caused by metal blockage on radio wave propagation predicated on the presence of vehicles as a subject of obstruction in comparison to obstacle-free vehicular environment. The validity of data is shown through received signal strength indicator (RSSI) and approximation analysis (RMSE) to demonstrate the efficiency of obtained measurements. The results demonstrated that Log-normal shadowing model yields the best fit to low-density metal obstruction scenario with smallest RMSE of 4.78 under bus obstruction whereas 5.72 under car obstruction.

Keywords: Metal obstruction, RF Propagation, RSSI, Vehicle obstruction, V2I Communication

1. INTRODUCTION

To date, the development of Intelligent Transportation System (ITS) radio communication has transcended the safety-related applications from sensing and detecting obstacles on the road into extending sensor's view by leveraging vehicle-to-everything (V2X) connectivity [1]. In fact, V2X resembles the ITS Connect [2] whereby in an ITS environment its traffic information, vehicles and pedestrians' whereabouts are generally broadcasted around junction areas via V2I mode. Such information exchange and transfer would involve small and large numbers of data including vehicle's location, directions, speed, video and maps amongst road-side-units (RSUs) and on-board-units (OBUs). Briefly, V2I communication plays an important role in vehicular communication and may assist connected cars by extending its communication range among vehicles within and out of range via ITS connect and or vehicular ad hoc network (VANET) [3].

---

* aziziharun@unimap.edu.my

In other words, V2I communication enables message transfer between RSU or base station and other mobile objects on the road or OBUs to provide safety warnings services for ITS applications as well as Connected Autonomous Vehicle (CAV). The term CAV is being used globally combining autonomous, connected cars, and advanced driver assistance systems (ADAS) technologies. Based on the driving standard [4], the autonomous vehicle can operate and control the basic driving function without direct input from the driver in self-driving mode. It can control the braking, steering, speed and aid the driver with route guidance via software or control algorithm which captures data from the secondary sensors such as ADAS, PCAM, HMI, GPS, radar and LiDAR, camera ultrasonic and many more. At present, most autonomous vehicles use both vision and radio-guided technologies [5]. In a real world scenario, a Giant Eagle Warehouse Company based in Pittsburgh accommodated Seegrid vision-guided autonomous forklifts for moving and carrying their product in a systematic order 24/7. They have maximized their productivity up to 30% and control the chaos in the workplace by integrating this autonomous vehicle alongside other robots, manned vehicles and pedestrian workers. This autonomous vehicle is installed with a large amount of data for their vehicle to operate in the most reliable, efficient ways and apart from that it has sensors for preventing accidents in the surroundings. In industrial applications, automatic guided vehicles (AGVs) are used to transport heavy materials and most of them today can be controlled both manually and automatically. Some are programmed to follow a particular lane with lines or wires on the floor. Others use radio waves, magnets, lasers and cameras for navigation purposes. For very similar reasons, the concept of V2I communication is implemented to autonomous features and into modern AGVs today so that accidents and costs can be reduced thus improving traffic efficiency in the workplace and on the road.

From wireless communication aspects, the propagation mechanism such as reflection, diffraction and scattering often affect radio wave and signal propagation over the cellular network [6]. Similarly, radio propagation in a vehicular communication environment may undergo a very unique and complex propagation which is characterized by different types of obstacles consists of buildings, vehicles and vegetation [7]. In the case of metal obstruction, radio wave propagation may be poorly speculated whereby in certain applications mainly in low density obstruction, minimum impact from metal object has not been considered. In fact, according to C. Tripp-Barba et al. [8], several radio propagation models being used in popular MANET simulators assume an obstacle-free environment and free line-of-sight (LOS) between communicating devices. This could result in unrealistic simulated scenarios in which simple radio propagation models usually overlooked the obstacles from the surrounding environment. Thus, assuming the performance of radio communication is LOS or free space is not sufficient. Signal will be varied by metal object regardless of the amount as the conductivity in metal is extremely high. The changes in amplitude at metal surface are abrupt and the thickness may completely block signal besides reflection [9]. As such, characterizing the metal effect on signal attenuation governing the signal propagation is imperative. To perform such characterization and analysis research was done accordingly to demonstrate the impact of low density metal obstruction in comparison to the obstacle-free environment on the basis of V2I mode. The application of this result could be used in smart robotic systems, autonomous vehicles, etc.

In the following sections, Section 2 describes related literature and research work as well as path loss propagation models. Measurement location and equipment are shown in Section 3 whereas the experimental designs and approach are illustrated in Section 4. The analysis, results and discussion are reported in Section 5. The findings of this research are concluded in Section 6.

2.   RESEARCH BACKGROUND

A number of previous literature and research work have demonstrated the effects of metal objects on radio propagation in regards to vehicular environment. In most studies, the impact of vehicular obstruction was analyzed according to V2V links in terms of its communication reliability [10], the impact from large vehicles [11] and the effect of vehicles in a variety of environments. Furthermore, the measurement campaign usually concentrated on moving cars and vehicle speed which clearly has negligible impact on signal attenuation [12]. In a vehicular environment, vehicles are always present at traffic light junctions, parking lots and highway in which safety warning applications is expected to improve traffic efficiency, speed as well as collision warning. These targeted areas are usually designated with V2I mode whereby the exchange of information occurs between the base station and vehicles to accommodate safety-related applications [13]. However, limited studies have been concentrating on V2I links which are generally characterized by multiple antenna heights for Tx or RSUs [14]. In our recent work, the presence of static cars on the parking lot area clearly shows differences in signal transmission range by 10 m and 15 m for 0.15 m as well as 1.3 m antenna height configuration, respectively [15]. This signifies that in V2I communication, it is also important to characterize radio propagation based on antenna heights besides its location and surrounding objects. Besides, a performance study was performed in a highway consisting of metal pillars which revealed that metallic environment affects RSU's antenna pattern [16]. A number of radio propagation models related to free space and obstacle obstruction that has been widely used in path loss predictions shall be described in subsection 2.1 below.

2.1   LOS and NLOS Path Loss Modelling

Fundamentally, there are several radio propagation models used for path loss prediction known as large-scale propagation and small-scale fading. These models are generally used for modeling vehicular obstruction in both line-of-sight (LOS) and non-line-of-sight (NLOS) conditions. For short range communication, RSSI is modelled using Log-Normal distribution [17]. When characterizing path loss models with RSSI measurement in LOS condition, Free Space Path Loss (FSPL) as given in equation (1) [6] is considered for path loss prediction under area free from physical obstruction.

$$\text{PL}_{\text{FSPL}}(\text{dB}) = -27.56 + 20\log_{10}(F) + 20\log_{10}(D) \tag{1}$$

where F is the frequency in MHz, D is the distance between the isotropic transmitting and receiving antennas in meters.

A distance-dependent path loss model known as Log-Distance Path Loss (LDPL) [6][15] model as given in equation (2) is often applied for modelling path loss by a number of researchers. LDPL model has been used to determine reference loss in NLOS communication links such as intersection centers [18], highway scenario [19], suburban area [20], multi-floor parking garage [21] as well as in rural environment. The improved version of LDPL, Dual Slope (DS) model [22] by Cheng et al. as given in equation (3) gives more accurate measurement data in suburban environment.

$$\text{PL}_{\text{LDPL}}(\text{dB}) = PL(D_0) + 10_N\log_{10}\frac{(D)}{D_0} + X_\sigma \tag{2}$$

$$\text{PL}_{\text{DS}}(\text{d}) = \begin{cases} PL(D_0) + 10N_1\log_{10}\left(\frac{D}{D_0}\right) + X_\sigma, & if\ D_0 \leq D \leq D_B \\ PL(D_0) + 10N_1\log_{10}\left(\frac{D_B}{D_0}\right) + 10N_2\log_{10}\left(\frac{D}{D_B}\right) + X_\sigma, & if\ D > D_B \end{cases} \tag{3}$$

where D_0 is the reference distance, D is the distance between transmitting Tx and receiving Rx antenna in meters. Path loss exponents, N are denoted by average attenuation in dB whereas $PL(D_0)$ represents the path loss reference D_0 in dB where $X\sigma$ is the zero-mean Gaussian distributed random variable with standard deviation, Both N_1 and N_2 are path loss exponents which reflects the scenario where power decays with path loss exponents and standard deviation until the breakpoint distance, D_B [15].

The measurement for LOS scenarios is usually preceded by traditional Two Ray model as observed in [11],[23]-[24] with the effort to model large vehicle obstructions via V2V communication links. The authors in [11] claimed that this model provides a reasonable fit after breakpoint distance in accordance with large vehicle impact. The breakpoint distance, D_B is used to distinguish the two ray propagation and diffraction region. Hence, equation (4) [11] can be applied to determine the distance from breakpoint to vehicle.

$$D_B = \left(\frac{h_{vehicle} - h_{OBU}}{h_{RSU}}\right) \times l_{vehicle} \tag{4}$$

where $h_{vehicle}$ and $l_{vehicle}$ represent the height and length of vehicle respectively, whereas h_{RSU} and h_{OBU} denote the height of transmitting antenna such as the RSU and OBU, respectively. The Two-Ray model that will be used for our measurement is given in equation (5) [15][25] which provides reasonable signal strength prediction over a distance of kilometers [26]. A complete Two-Ray model which considers small Tx-Rx separation is given in equation (13) in [27].

$$PL_{2RAY}(dB) = 40 \log D - (10 \log G_T + 10 \log G_R + 20 \log H_T + 20 \log H_R) \tag{5}$$

where D is the distance between Tx-Tr in meters, G_T and G_R represent transmitting and receiving antenna gain = 1, H_T and H_R are transmitting and receiving antenna heights in meters, respectively.

3. MEASUREMENT LOCATION AND EQUIPMENT

The channel measurement is conducted using XBEE S2C RF modules [28], wireless sensor nodes denoting coordinator as the Rx and remote as Tx. Based on the real-world scenario, Rx resembles the RSU, base station, hotspot or traffic light whereas Tx resembles the mobile objects on the road, OBUs. The Tx node is programmed as a remote device while Rx is programmed as local that is connected to a laptop with XCTU software [29] installed. The XCTU software from Digi XBEE can measure RSSI (dBm) of each Tx and Rx node. Basically, it is a one-way communication from Tx to Rx to denote V2I links. This device operates at 2.4 GHz ISM frequency band with 3 dB antenna gain. The receiver sensitivity description is -100 dBm based on XBEE S2C specification in [28].

Throughout the measurement campaign, the experimental setup and data collection are held entirely in Universiti Malaysia Perlis campus area. The setup took place on three separate locations for both LOS and NLOS scenarios that is UniMAP Racing Circuit, student's hostel car parking lot and UniMAP student shuttle bus station as shown in Figure 1. For LOS scenario, the location from Figure 1 (a) is assumed free from obstacles hence this environment is applied for baseline measurement with no metal obstruction presence nearby Fresnel Zone [30]. For NLOS environment shown in Figure 1(b) consist of a single row of cars parked side-by-side in a car parking lot area and likewise the buses in UniMAP's bus station are as shown in Figure 1 (c). Based on these Figures, D is the maximum distance between transmitting and receiving antenna, D_1 denoting initial reference distance in meter whereas D_n represents the number of reference points for D, with n = 0,1,2,3…n.
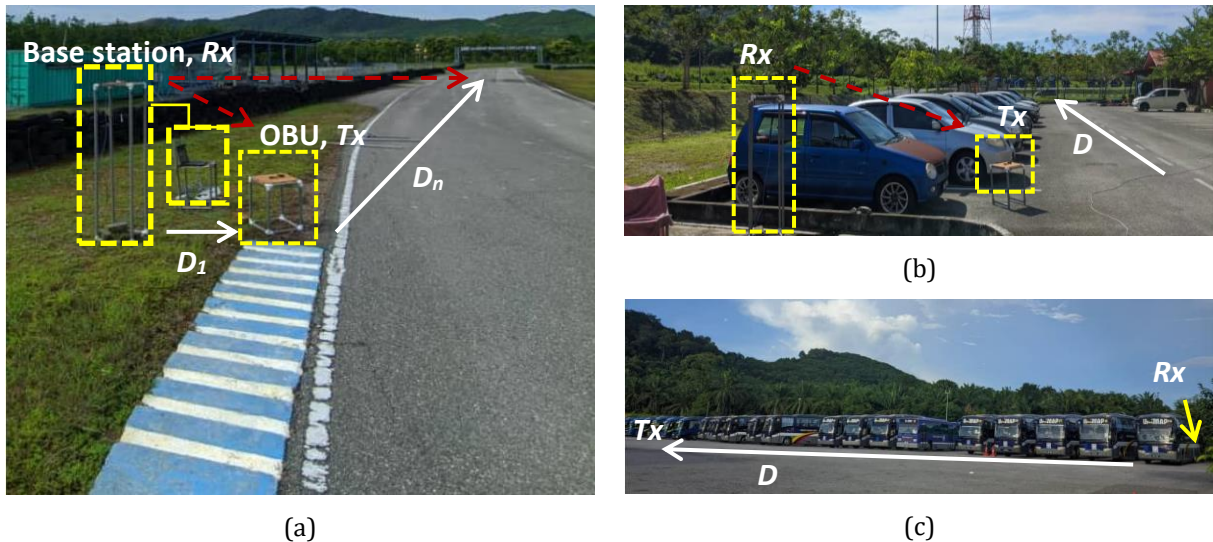
Figure 1. Measurement Campaign at (a) UniMAP Racing Circuit, (b) student's hostel car park, (c) UniMAP bus station with *Rx* is referring to Base Station, *Tx* as Mobile Unit and *D* is distance.

4. EXPERIMENTAL DESIGN AND APPROACH

Before the channel measurement is performed on each location, 1st Fresnel Zone is calculated and XCTU spectrum analyzer is used to measure the radio band in the vicinity. This is to ensure that measurements can be conducted in utmost performance whereby unnecessary interference has been avoided. The experimental setup is focused on static metal obstacles within V2I communication channel in two categories. The first category is conducted in an LOS environment whereby the setup is without presence of obstacles nearby Fresnel Zone Clearance Radius, R [27][30] as well as in between the transmitting and receiving antennas. Likewise, the second category is conducted on two separate parking lots consisting cars and buses in a row. The latter scenario is referring to NLOS environments because on each parking lot, the metal obstacle is present in between the transmitting and receiving antennas. The illustration of each LOS and NLOS measurement setup with transmitting and receiving antennas is as depicted in Figure 2 (a) and (b), respectively.
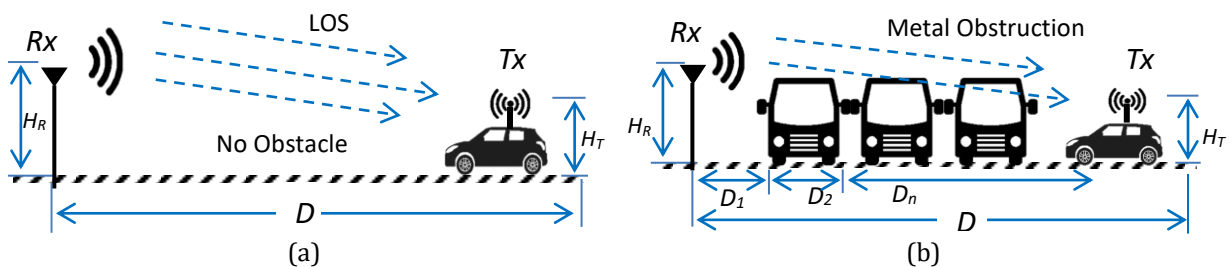
Figure 2. Channel measurement setup under (a) LOS scenario with free-way road and (b) NLOS scenario consisting metal object in between transmitting, *Tx* and receiving, *Rx* antennas.

The metal obstruction as illustrated in Figure 2 (b) is referring to the presence of bus and car. These vehicles are regarded as metallic object since in automotive industry the manufacture of car bodies consists mostly of cast iron and steel [31]. For NLOS scenario setup, twelve cars were parked in single row between transmitting and receiving antennas. The standard height of car from its rooftop is 1.5 m with body width of 4.4 m. For the bus, twenty buses were present in that parking lot with 3 m height and body width of 10 m. The maximum depth or distance, *D*

that the signal travels through the metal object is approximately 50 m which is similar to maximum length of vehicles present.

The setup of transmitting and receiving antennas for both LOS and NLOS scenarios involves three antenna heights configuration to represent both V2I links concept. In each scenario, *Rx* is allocated as base station (RSU) at 3.5 m antenna height. Three different heights for *Tx* that is 0.5 m, 1.5 m and 3.0 m resemble the handheld device, car and bus, respectively. The description of multiple antenna height configurations is given in Table 1.

Table 1 Antenna height configuration for LOS and NLOS scenarios

Communication Mode	Scenario/Object	Antenna Heights (m)					
		LOS		Car		Bus	
		Rx	*Tx*	*Rx*	*Tx*	*Rx*	*Tx*
V2I	**RSU-Handheld**	3.5	0.5	3.5	0.5	3.5	0.5
	RSU-Car	3.5	1.5	3.5	1.5	3.5	1.5
	RSU-Bus	3.5	3.0	3.5	3.0	3.5	3.0

The *Rx* is specified to 3.5 m to resemble a typical RSU or base station height installed on the roadside whereas *Tx* height is specified at 0.5 m, 1.5 m and 3.0 m constituting the OBUs (see Table 1). In a microcell environment, the base station is usually placed below the rooftop level [32] in which the communication between V2I links normally occurs between the base station and handheld devices as well as vehicles. The standard height for *Rx* and *Tx* that is applicable for predicting LOS between frequency range of 0.4 to 6 GHz is about 0.5 to 3.5 m [33], thus our specification of RSU and OBU height follows this standard validation parameters at 2.4 GHz.

Each *Tx* and *Rx* node is placed on top of plastic poles that can be adjusted to represent vehicle's heights. The pole is preferred compared to actual vehicle to avoid unnecessary interference due to nearby metal object that may obstruct the Fresnel Zone of the *Tx* node. This way, channel measurement can be performed with optimum performance. During data collection, the *Rx* antenna is connected to a laptop and runs on power supply. The *Rx* works as base station or RSU thus it is positioned in a fixed location throughout the entire experiment on each location. *Tx* node is positioned at allocated distance, D_n (see Figure 2 b). The interval distance from Rx node begins at 1 m increment from D_1 to D_{10}, 2 m increment from D_{10} to D_{20} and 5 m increment from D_{20} to D_{50}. The maximum distance acquired is 50 m. At each point, signal is transmitted up to 2 minutes with 1 packet per second. The signal transmission is repeated two times whereby the RSSI values in dBm is recorded and averaged at each point.

5. RESULTS AND DISCUSSION

In this section, results are demonstrated into three separate parts. First, signal attenuation profile in terms of RSSI (dBm) is illustrated based on clear LOS and low density metal obstructions from car and bus. Secondly, LOS and NLOS path loss models such as Log-normal shadowing model, Log-distance, Two Ray and Cheng Dual Slope are fitted into our measurement data for three different OBUs configuration heights. Third, RMSE values obtained from both LOS path loss modelling, car and bus attenuation profile modelling are summarized.

5.1 RSSI

The signal attenuation profile of LOS scenario, car and bus obstructions based on antenna height configuration as *Rx* x *Tx* of 3.5 m x 0.5 m, 3.5 m x 1.5 m and 3.5 m x 3.0 m are as illustrated in

Figure 3, 4 and 5, respectively. Based on Figure 3, RSSI values started at -44 dBm and gradually decreased after 4 m until 10 m distance with car obstruction. After 10 m the signal fluctuated and ascended until 25 m before gradually fluctuated towards 50 m. With bus obstruction starting at -52 dBm signal fluctuates drastically up to 6 m. Large signal attenuation is observed from the baseline at 7 m as it continues to descend until 50 m (-78 dBm) distance.
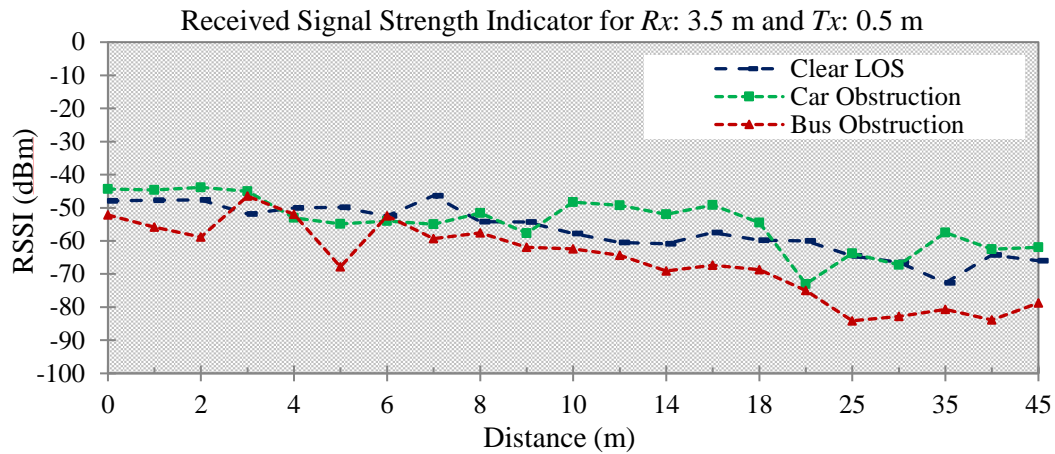
Figure 3. Attenuation profile for LOS, car and bus obstruction at 3.5 x 0.5 m antenna height.

Based on Figure 4, the results show that RSSI values decrease to -58 dBm for both car and bus at 1 meter start. The attenuation profile for car increased to -48 dBm at 5 m before gradually fluctuates in descending manner until 50 m. Whereas the attenuation profile for bus fluctuates in similar manner for first 12 m distance before decreasing until 18 m (-75 dBm). The signal experience abrupt increase at 20 m (-63 dBm) before attenuated farther from the baseline up to 50 m distance with RSSI level -78 dBm.
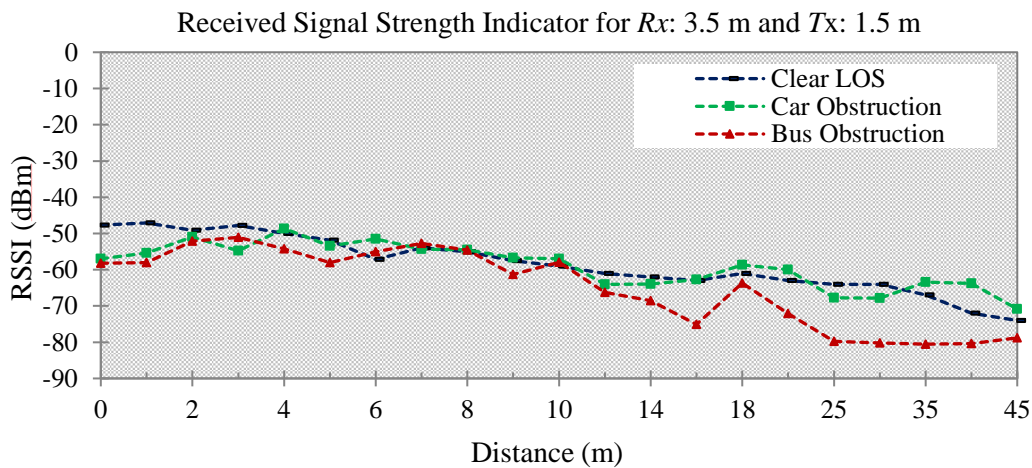
Figure 4. Attenuation profile for LOS, car and bus obstruction at 3.5 x 1.5 m antenna height.

Figure 5 shows that the signal fluctuated mildly for both car and bus obstruction. However, large signal attenuation is observed with bus obstructions starting at 18 m distance towards 50 m with RSSI level reduced from -59 dBm to -78 dBm. As the height of *Tx* is increased to 3.0 m, the signal able to propagate with minimal fluctuation from the baseline before undergoes drastic attenuation starting at 20 m till 50 m. Fair signal fluctuations is observed with car obstruction up to 25 m distance with RSSI level starting at – 35 dBm and ended with – 58 dBm at 50 m distance. Instant fluctuations occurred at 40 m towards 50 m distance which shows that

signal can still propagate to a greater distance due to antenna height configuration which allows clearer and unobstructed path for signal to travel through car obstruction. For bus obstruction, the signal is significantly affected after 20 m distance which shows that although having *Tx* height of similar level, the presence of large metal object may still affect the signal power.
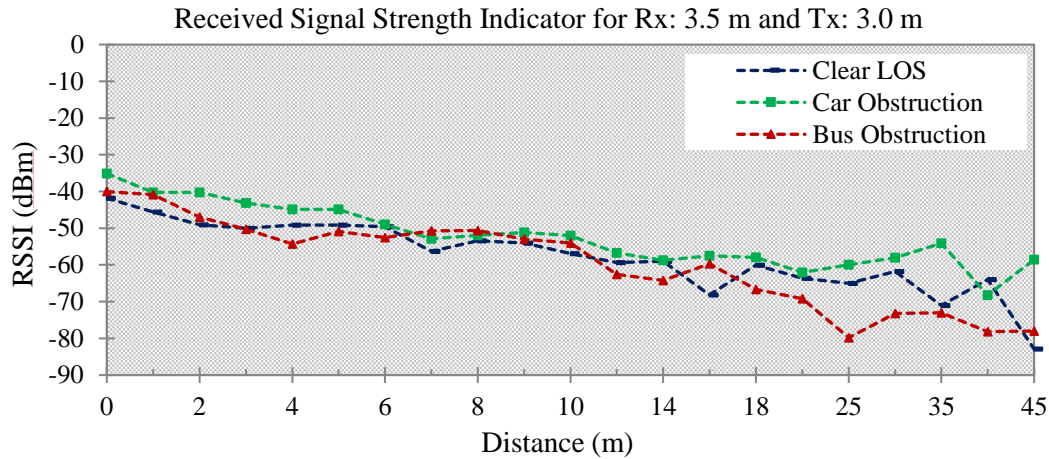
Figure 5. Attenuation profile for LOS, car and bus obstruction at 3.5 x 3.0 m antenna height.

The high level of attenuation may be caused by several factors such as antenna heights, ground effect and presence of metal object. The Fresnel Zone Clearance Radius, *R* suggests that the maximum allowable obstruction for antenna heights must be at least 1 m for a maximum distance of 50 m. Since *Tx* height is 0.5 m above the ground, the effect from ground surface has contributed to signal reflection hence causing signal to experience multipath effect.

The distance between transmitting and receiving antennas also contribute to signal power reduction over distance. As distance increases, the RSSI level will decrease monotonically until *Rx* or *Tx* reaches its sensitivity limit regardless of changes in antenna heights. Knowing the maximum coverage distance of base station at a specific location is necessary for accessing the reliability both in communication and application wise. In real-world applications, some neighboring RSUs can be found installed every 2 - 3 km [3] to provide coverage via V2I links. Certain applications rely on short distance outdoor communication less than 1 km with at least 2-10 m antenna height [34]. This type of communication mode is suitable for junction and road intersection with traffic lights which is vital in ITS Connect environment given that antenna height installation is in accordance to location and its purpose for optimum coverage. For instance, the requirement range for V2I and V2V communication-based safety applications for safety warning services is specified from 50 m up to 300 m depending on different types of safety alerts [13].

The reflection caused by metal surface is another prominent factor to signal level diminution. By rule of thumb, the reflection angle equals incidence angle over a metal surface which is predicated on metal thickness and skin depth, δ (micron) [9]. This is because metal object is high in conductivity and generally transmitted signal may occur at shorter distance than wavelength. The changes in signal amplitude may be abrupt and if the metal surface thickness is larger than skin depth then signal may not be able to penetrate the surface. Rather if the object is larger than the wavelength, diffraction occurs which in this case is similar to car obstruction. The signal may still travel to a greater distance even with presence of twelve cars blocking the LOS. However, with larger metal object obstruction such as bus the transmitted signal may experience reflection by metals at certain distance and based on our results it clearly shows a significant drop in RSSI starting at 30 m regardless of antenna height configurations. With that,

these attenuation profiles are modelled with predicted path loss models to validate and determine best fit when modelled against our measurement data.

5.2   PATH LOSS MODELLING

The comparisons of LOS and NLOS path loss models are as depicted in Figure 6 and Figure 7. From the top to bottom view, Figure 6 from on the left hand shows the attenuation profile when modelled with path loss models in the basis of car obstruction whereas Figure 7 on the right hand shows the results with bus obstruction in accordance to (a) 3.5 x 0.5 m, (b) 3.5 x 1.5 m and (c) 3.5 x 3.0 m antenna heights configuration. Based on Figure 6 (a), Log-normal shadowing model gives RMSE value of 9.86 followed by Two Ray with 12.03, Cheng's Dual Slope 21.17 and Log-Distance is 23.52. When *Tx* height is increased to 1.5 m as, the Log-Normal shadowing shows an increase in RMSE value up to 17.00 as shown in Figure 6(b). The RMSE value of each path loss model is reduced slightly indicating a better profile fit to our measurement data by Cheng's dual slope with 17.39, Two-Ray with 17.50 and Log-distance with 17.88. From Figure 6 (c), with *Tx* height is increased to 3.0 m, the distribution of Log-normal yields the smallest RMSE value that is 5.72 followed by Two-Ray which is 12.45, Cheng's slope with 23.83, and Log-Distance 30.29. The Log-normal shows a more accurate fit when model against car obstruction at 3.5 x 3.0 m whereas Two-Ray model shows better fit at both 3.5 x 0.5 m and 3.5 x 3.0 m antenna height configurations. On the contrary, a fair fit can be observed when modelling against 3.5 x 1.5 m antenna height. The summary of RMSE values under car obstruction is as shown in Table 2.

(a)

(a)

(b)

(b)
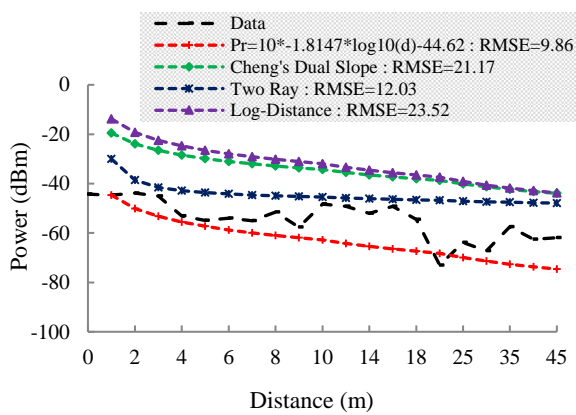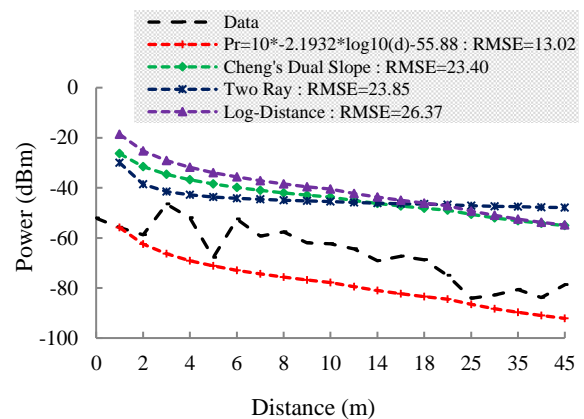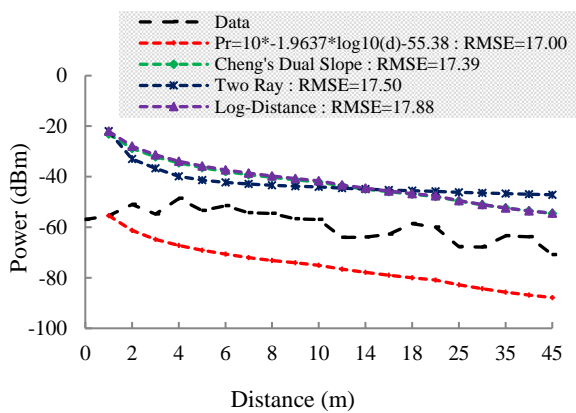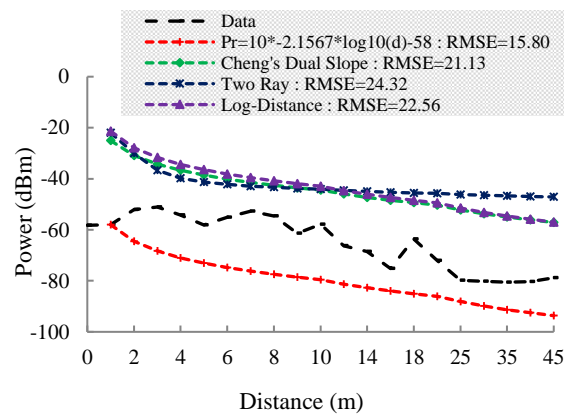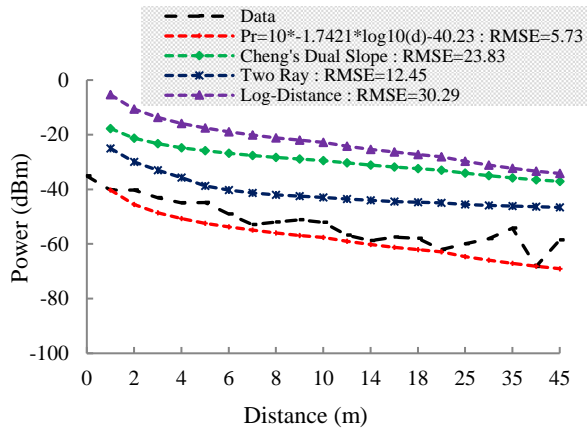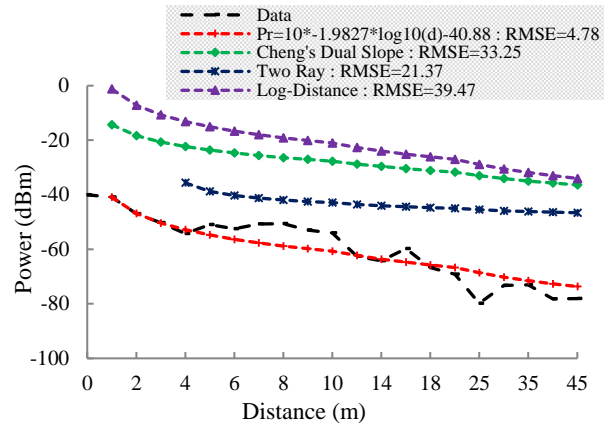
Figure 6. Path loss modelling of attenuation profile with car obstruction at (a) 3.5 x 0.5 m, (b) 3.5 x 1.5 m and (c) 3.5 x 0.5 m antenna height.

Figure 7. Path loss modelling of attenuation profile with bus obstruction at (a) 3.5 x 0.5 m, (b) 3.5 x 1.5 m and (c) 3.5 x 0.5 m antenna height.

Table 2 RMSE of Path Loss Models with Car Obstruction

Antenna Height (m)	Log-Normal (dB)	Log-Distance (dB)	Cheng Dual Slope (dB)	Two Ray (dB)
3.5 m x 0.5 m	9.86	23.52	21.17	12.03
3.5 m x 1.5 m	17.00	17.88	17.39	17.50
3.5 m x 3.0 m	5.72	30.29	23.83	12.45

Based on Figure 7, the RMSE values under bus obstruction are larger for all three *Tx* antenna heights configuration when modelled using Log-Distance, Cheng Dual Slope and Two Ray which yield RMSE of 26.37, 23.40 and 23.85 at 3.5 x 0.5 m as in Figure 7 (a). When modelled at 3.5 x 1.5 m antenna height the RMSE values obtained is 22.56, 21.13 and 24.32 from Log-Distance, Cheng Dual Slope and Two-Ray, respectively as shown in Figure 7 (b) whereas at higher *Tx* antenna height configuration 3.0 m as in Figure 7 (c), The RMSE values are 39.47, 33.25 and 21.37. Modelling Log-Normal model against 3.5 x 3.0 m gives the smallest RMSE, 4.78 followed by 13.02 and 15.8 at 3.5 x 0.5 m and 3.5 x 1.5 m, respectively. The summary of RMSE under bus obstruction is as shown in Table 3. Based on our observation, Log-Normal shadowing model shows a more accurate fit when modelled against 3.5 x 3.0 m with bus obstruction whereas Log-distance and Cheng Dual Slope yield large RMSE of 39.47 and 33.25, respectively. Although Two-Ray model shows a fair RMSE values under both LOS and NLOS scenarios, this model only follows normal distribution beginning at 5 m when modelled against bus obstruction at 3.5 x 3.0 m.

Table 3 RMSE of Path Loss Models with Bus Obstruction

Antenna Height (m)	Log-Normal (dB)	Log-Distance (dB)	Cheng Dual Slope (dB)	Two Ray (dB)
3.5 m x 0.5 m	13.02	26.37	23.40	23.85
3.5 m x 1.5 m	15.80	22.56	21.13	24.32
3.5 m x 3.0 m	4.78	39.47	33.25	21.37

6. CONCLUSION

The impact of metal object on signal strength based on of real-world measurement in the basis of low density vehicle obstruction in comparison to obstacle-free environment has been demonstrated in this paper. The attenuation profile has been described and validated with predicted path loss models. The analysis shows that Log-Normal shadowing yields the least error which indicates that it has the best fit for both LOS and NLOS scenario with respect to metal obstruction. Nevertheless, Two-Ray model may be applied in a vehicular environment consisting cars as the RMSE yields consistent fit to the measurement data under car obstruction. However, the errors from Log-Distance path loss models including Cheng Dual Slope shows inconsistency in RMSE values when modelling under car and bus obstruction environment. Furthermore, Two-Ray model is shown to be effective and has been used in comparison to a new and improved proposed models other than Free Space Loss and CORNER models in various literatures related to obstacle modelling under V2V mode. The findings from this research work could provide important input parameters and may assist on designing vehicular channel under V2I mode in our future work.

ACKNOWLEDGEMENTS

REFERENCES

[1] R. Popescu-Zeletin, I. Radusch, M. A. Rigani, "Vehicular-2-X Communication," in State-of-the-Art Research in Mob. Vehic. Ad hoc Netw., Berlin, Germany: Springer, (2010)

[2] Report ITU-R M.2445-0 Intelligent Transport Systems (ITS) Usage, (2018) pp. 223-234.

[3] Mershad K., Artail H., Gerla M., Ad Hoc Networks. ROAMER : Roadside Units as message routers in VANETs. vol **10,** (2012) pp. 479–496.

[4] D. Ticoll, "Driving Changes: Automated Vehicles in Toronto," Toronto: Discuss. Paper UTTRI, (2015) p 67.

[5] K. Bimbraw, "Autonomous Cars : Past , Present and Future," in 12th Int. Conf. Informatics Control. Autom. Robot., vol **1,** (2015) pp. 191–198.

[6] T. S. Rappaport, "Wireless Communication: Principles and Practice," 2nd Edi. NJ: Prentice Hall PTR, (2002) pp. 107-109

[7] W. Viriyasitavat, M. Boban, H. M. Tsai, A. Vasilakos, "Vehicular communications: Survey and challenges of channel and propagation models," in IEEE Veh. Technol. Mag., vol **10,** (2015) pp. 55–66.

[8] Tripp-barba C, Urquiza-aguiar L, Zaldívar-colado A, Estrada-jiménez J., Aguilar-calderón J. A., Aguilar M., Veh. Commun. Comparison of propagation and packet error models in vehicular networks performance. vol **12,** (2018) pp. 1–13.

[9] D. M. Dobkin, "RF Engineering for Wireless Networks," USA: Elsevier Inc., (2005)

[10] T. Zinchenko, L. Wolf, M. Fidler, "Reliability Assessment of Vehicle-to-Vehicle Communication," Dr.-Ing Dissertation, Technische Universitat Braunschweig, (2014)

[11] He R., Molisch A. F., Tufvesson F., Zhong Z., Ai B., Zhang T., IEEE Trans. Intell. Transp. Sys. Vehicle-to-Vehicle Propagation Models With Large Vehicle Obstructions. vol **15,** (2014) pp. 2237–2248.

[12] Qureshi M. A., Noor R., Shamim A., Shamshirband S. Choo K. R., J. Plus One. A Lightweight Radio Propagation Model for Vehicular Communication in Road Tunnels.(2016) pp. 1–15.

[13] Singh P. K., Nandi S. K., Nandi S., Veh. Commun. A tutorial survey on vehicular communication state of the art, and future research directions. vol **18,** (2019) p 100164.

[14] Yi H., Guan K., He D., Ai B., Dou J. Kim J., IEEE Access J. Special Sec. Millim.-wave Terahertz Propag., Chan. Model. and App. Characterization for the Vehicle-to-Infrastructure Channel in Urban and Highway Scenarios at the Terahertz Band. vol **7,** (2019) pp. 166984-166996.

[15] J. S. C. Turner et al., "Modeling on impact of metal object obstruction in urban environment for internet of things application in vehicular communication," in The 2nd International Conference on Applied Photonics and Electronics (InCAPE), A I P Conf. Proc., Malaysia, vol **2203,** (2020) p 020053.

[16] A. Paier, R. Tresch, A. Alonso, D. Smely, P. Meckel, Y. Zhou, N. Czink, "Average Downstream Performance of Measured IEEE 802.11p Infrastructure-to-Vehicle Links," in IEEE Int. Conf. Commun. Work. ICC, (2010) pp. 1–5.

[17] Ndzi D. L., Arif M. A. M., Shakaff A. Y. M., Ahmad M. N., Harun A., Kamarudin L. M., Zakaria A., Ramli M. F., Razalli, Prog. Electromagn. Res. Signal Propagation Analysis for Low Data Rate Wireless Sensor Network Applications in Sport Grounds and on Roads.vol **125,** (2012) pp. 1–19.

[18] Mangel T., Klemp O., Hartenstein H., EURASIP J. Wireless Commun. Netw. 5.9 GHz inter-vehicle communication at intersections: a validated non-line-of-sight path-loss and fading model. vol **2011**, issue 1 (2011) p 182.

[19] Abbas T., Sjoberg K., Karedal J., Tufvesson F., Int. J. Ant and Propag. Shadow Fading Model for Vehicle-to-Vehicle Network Simulations. vol **2015,** (2015) p 12.

[20] Cheng L., Henty B. E., Stancil D. D., Bai F., Mudalige P., IEEE J. Sel. Areas Commun. Mobile vehicle-to-vehicle narrow-band channel measurement and characterization of the 5.9 GHz Dedicated Short Range Communication (DSRC) frequency band. vol **25**, (2007) pp. 1501–1516.

[21] R. Sun, D. W. Matolak, P. Liu, "Parking Garage Channel Characteristics at 5 GHz for V2V Applications," in IEEE 78th Veh. Technol. Conf. VTC Fall, (2013) pp. 1–5.

[22] J. S. C. Turner *et al.,* "Modelling on Impact of Building Obstruction for V2I Communication Link in Micro Cellular Environment," in 5th International Conference on Electronic Design (ICED), J. Phys. Conf. Ser., vol **1755,** (2021).

[23] J. Karedal, N. Czink, A. Paier, F. Tufvesson, A. F. Molisch, "Path Loss Modeling for Vehicle-to-Vehicle Communications," in IEEE Trans. on Vehicular Tech. vol **60,** issue 1 (2011) pp. 323–328.

[24] M. Boban, J. Barros, O. K. Tonguz, "Geometry-based vehicle-to-vehicle channel modeling for large-scale simulation," in IEEE Trans. Veh. Technol. vol **63,** (2014) pp. 4146–4164.

[25] A. Harun, A. Y. M. Shakaff, A. Zakaria, L. M. Kamarudin, M. N. Jaafar, D. L. Ndzi, "Wireless sensor networks mapping and deployment in tropical precision farming," in Proc. - CIMSim 3rd Int. Conf. Comput. Intell. Model. Simul. 2011 pp 346–350.

[26] Jha C. K., Jain R., Int. J. of Sci. and Res. Literature Survey on Various Outdoor Propagation Model for Fixed Wireless Network. vol **3,** issue 8 (2014) pp. 2012–2015.

[27] J. S. C. Turner et al., "Effect of Roadways Plantation on Signal Propagation Analysis in Connected Autonomous Vehicle Communication," in IOP Conf. Ser. Mater. Sci. Eng., vol **557,** (2019) p 012056.

[28] Digi Xbee S2C 802.15.4 RF Modules, Digi International, (2017).

[29] Configuration and Test Utility Software, XCTU Manual, XCTU User Guide, Digi International Inc. All rights reserved, (2019).

[30] J. S. C. Turner, A. B. Shahriman, A. Harun, Z. M. Razlan, M. S. M. Hashim, W. K. Wan, M. A. Fadzilla, S. A. Z. Murad, N. A. M. A. Hambali, C. Y. Phoon, "Modeling Effect of Road Topology on Signal Analysis in Connected Autonomous Vehicle Communication," in 5th International Conference on Man Machine Systems Ser. I O P Conf. Sci. Mater. vol **705,** (2019) p 012053.

[31] Hovorun T. P., Berladir K. V., Pererva V. I., Rudenko S. G., Martynov A. I., J. of Eng. Sci. Modern materials for automotive industry. vol **4,** issue 2 (2017) pp. f8-f18.

[32] Propagation data and prediction methods for the planning of short-range outdoor radiocommunication systems and radio local area networks in the frequency range 300 MHz to 100 GHz, Recommendation ITU-R P.1411-10, P Series, Radiowave propagation, (2019).

[33] Y. Ito, T. Taga, J. Muramatsu, N. Suzuki, "Prediction of Line-Of-Sight Propagation Loss in Inter-Vehicle Communication Environments," in 18th Annual IEEE Int.Symp. on Personal, Indoor and Mobile Radio Commun., (2007).

[34] S. K. Noh, P. J. Kim, J. H. Yoon, "Doppler Effect on V2I Path Loss and V2V Channel Models," in Int. Conf. Inf. Commun. Technol. Converg., (2016) pp. 898–902.